

## Remote Sensing-Based Deep Learning Approach for Identifying Burned Forest Areas

Reha PAŞAOĞLU<sup>1,a</sup>, Ahmet Ertuğrul ARIK<sup>1,b</sup>, Nuri EMRAHOĞLU<sup>1,c</sup>

<sup>1</sup>Osmaniye Korkutata University, Kadirli Vocational School, Osmaniye, Türkiye

<sup>a</sup>ORCID: 0000-0002-4260-5468; <sup>b</sup>ORCID: 0000-0002-7952-4311; <sup>c</sup>ORCID: 0000-0003-4347-5279

### Article Info

Received : 18.09.2024

Accepted : 25.03.2025

DOI: 10.21605/cukurovaumfd.1665481

### Corresponding Author

Ahmet Ertuğrul ARIK

ertugrul.arik@kapadokya.edu.tr

### Keywords

Deep learning

Sentinel 2

NBR-dNBR

BAIS2-dBAIS2

Remote sensing

**How to cite:** PAŞAOĞLU, R., ARIK, A.E., EMRAHOĞLU, N., (2025). Remote Sensing-Based Deep Learning Approach for Identifying Burned Forest Areas. Cukurova University, Journal of the Faculty of Engineering, 40(1), 33-48.

### ABSTRACT

In this study, the burned areas and intensity of forest fires that occurred in the Samandağ region of Hatay between September 5-10, 2020, are mapped. Analyses were carried out using deep learning, remote sensing, and satellite data from Sentinel 2. With Sentinel 2 satellite photos of the research locations, an image dataset for deep learning was constructed. Then, using deep learning approaches, a deep learning model was developed, trained using the photos in the dataset, and successfully tested. Images from Sentinel 2 were used to produce the Normalized Burn Ratio(NBR) and Burned Area Index for Sentinel 2 (BAIS2) indices using the results of a new deep learning model. Calculating the Difference Normalized Burning Intensity (dNBR) and Burned Area Index for Difference Sentinel-2 (dBAIS2) values for the discrepancies between these indices before and after the fire allowed for categorization and determination of the fire area. The deep learning approach burned area indexes, and General Directorate of Forestry (GDF) fire registration slips were compared, and it was established that the new deep learning model was more effective at locating burned forest areas than the indexes. In identifying the burnt forest areas, the new model has a proportionate accuracy of 98.36% in the Samandağ study region.

## Yanmış Orman Alanlarının Belirlenmesi için Uzaktan Algılama Tabanlı Derin Öğrenme Yaklaşımı

### Makale Bilgileri

Geliş : 18.09.2024

Kabul : 25.03.2025

DOI: 10.21605/cukurovaumfd.1665481

### Sorumlu Yazar

Ahmet Ertuğrul ARIK

ertugrul.arik@kapadokya.edu.tr

### Anahtar Kelimeler

Derin öğrenme

Sentinel 2

NBR-dNBR

BAIS2-dBAIS2

Uzaktan algılama

**Atf şekli:** PAŞAOĞLU, R., ARIK, A.E., EMRAHOĞLU, N., (2025). Yanmış Orman Alanlarının Belirlenmesi için Uzaktan Algılama Tabanlı Derin Öğrenme Yaklaşımı. Çukurova Üniversitesi, Mühendislik Fakültesi Dergisi, 40(1), 33-48.

### ÖZ

Bu çalışmada, 5-10 Eylül 2020 tarihleri arasında Hatay'ın Samandağ bölgesinde meydana gelen orman yangınlarının yanık alanları ve şiddeti haritalandırılmıştır. Derin öğrenme, uzaktan algılama ve Sentinel 2 uydu verileri kullanılarak analizler yapılmıştır. Araştırma bölgelerine ait Sentinel 2 uydu fotoğrafları ile derin öğrenme için bir görüntü veri seti oluşturulmuştur. Ardından, derin öğrenme yaklaşımları kullanılarak bir model geliştirilmiş, bu model veri setindeki fotoğraflarla eğitilmiş ve başarıyla test edilmiştir. Sentinel 2'den elde edilen görüntüler, yeni derin öğrenme modelinin sonuçları kullanılarak Normalleştirilmiş Yanma Yoğunluğu (NBR) ve Yanık Alan İndeksi (BAIS2) değerleri hesaplanmıştır. Yangın öncesi ve sonrası bu indeksler arasındaki farklılıkların hesaplanmasıyla Farklı Normalleştirilmiş Yanma Yoğunluğu (dNBR) ve Farklı Yanık Alan İndeksi (dBAIS2) değerleri elde edilerek yangın alanı kategorize edilmiş ve belirlenmiştir. Derin öğrenme yaklaşımı, yanık alan indeksleri ve Orman Genel Müdürlüğü yangın kayıt fişleri karşılaştırılmış ve yeni derin öğrenme modelinin yanmış orman alanlarını belirlemede indekslere göre daha etkili olduğu tespit edilmiştir. Samandağ çalışma bölgesinde, yanık orman alanlarının belirlenmesinde yeni modelin doğruluk oranı %98,36 olarak hesaplanmıştır.

## 1. INTRODUCTION

This article is based on the findings of the thesis titled 'Comparison of Deep Learning Methods with Burned Area Indices in the Detection of Burned Forest Areas: The Case of Hatay.

Forest fires are among the natural events that most significantly affect the global ecosystem. While the incidence of fires has increased due to environmental climate changes, many fires are human-induced. The rise in the world's population has led to increased utilization of forest areas and a higher demand for forest products. Forest fires cause considerable damage to the geographies in which they occur and negatively impact all life forms. With climate changes, air temperatures are now frequently exceeding average levels compared to previous years, creating favorable conditions for forest fires. In a world where global warming has reduced precipitation and led to the formation of deserts, forest fires pose a significant threat to our ecosystem. According to the most recent statistics, the annual loss of forest area due to fires has risen to 13 million hectares [1] In our country, only 1.6% of the total 27 million hectares of forest area is protected [2].

On the other hand, the ecology of the Mediterranean basin has developed significant resilience against severe forest fires. In recent years, there has been an increase in the number of forest fires, which has the potential to disrupt this balance [3]. Forest fires are one of the most serious dangers threatening natural life and are a major cause of economic losses due to the disruption of forestry activities. Additionally, forest fires are a significant source of air pollution.

Fires have the potential to adversely affect the natural environment, including flora, water, and air. They not only damage the forests in the vicinity but also threaten homes and farms in the area, causing both human and material losses [4]. The increase in forest fires complicates fieldwork, hence remote sensing techniques are crucial for identifying burned forest areas and formulating an emergency strategy.

The detection and analysis of such fire-affected areas are critical for implementing accurate policies swiftly. Consequently, the use of remote sensing methods has gained significant importance in recent years due to their speed and cost-effectiveness in detection and data collection, becoming increasingly widespread. Remote sensing is a crucial factor in the detection and analysis of forest fires. In countries with vast territories like Australia and Russia, identifying fires or determining burn rates using traditional methods is very challenging and time-consuming. Therefore, remote sensing is the fastest method for assessing forest fires. Any type of earth observation tool capable of collecting data can be used in remote sensing; this tool could be an aircraft, satellite, or UAV.

The use of aircraft in remote sensing methods for fighting forest fires can be extremely advantageous from many different aspects, from coordinating tactical operations and extinguishing activities to the rapid evacuation of the injured and the transport of personnel and materials. In Turkey, forest fires are a common occurrence during the summer months, especially in regions surrounding the Mediterranean and Aegean seas. Given the magnitudes of recent fires, disaster management requires meticulous attention [5].

In recent years, satellites have been extensively used for fire detection and analysis [6,7]. Satellites possess multiple and wide-range bands, enabling them to perform object classification based on different spectral reflectance values. The reflected radiation values from healthy vegetation, burned forest areas, soil, or water are distinct. Consequently, forest fires can be easily detected through certain calculations. Indices that identify burning or burned areas can be utilized in detection and analysis processes.

Furthermore, with the advancement of computer learning methods like deep learning, fire detection and analysis operations have become faster and have shifted towards these technologies. Deep learning techniques leverage the multi-spectral data provided by satellites to effectively distinguish between burned and unburned areas, enhancing the accuracy and efficiency of fire mapping. These advancements not only improve response times but also help in better management and recovery planning in post-fire scenarios.

## 2. RELATED STUDIES

In the past, burned forest areas were identified using ground surveys and maps; however, fires can now be rapidly monitored worldwide through remote sensing techniques [8].

Key and colleagues [9] developed a new index called the Normalized Burn Ratio (NBR) using bands 4 and 7 from Landsat TM data. This index was applied to data from two fires in Montana's Glacier National Park in 1994, and it was found that NBR was more successful in detecting burn severity compared to the Composite Burn Index (CBI).

Miller et al. [10] introduced the Difference Normalized Burn Ratio (dNBR) for mapping the burn severity of forest areas. This index was tested on 14 fires in California, USA, and its effectiveness was confirmed.

Filipponi [11] developed a new burned area detection index for Sentinel-2 data. This new index was applied to a fire in Sicily, Italy, in 2017 and was found to be more successful than the NBR index.

Mpakairi et al. [12] used six commonly employed indices along with Landsat 8-OLI data for two fires in northwestern Zimbabwe and classified them using the Random Forest (RF) machine learning algorithm. The Optimized Soil Adjusted Vegetation Index (OSAVI) and Normalized Burn Index (NBI) performed much better than any other spectral indices considered at both research locations. The Burned Area Index (BAI) was the third best performing spectral index. Both OSAVI and NBI showed better performance due to adjustments made for soil effects and the inclusion of the blue spectral band to account for atmospheric effects.

Tanasse et al. [13] developed a locally adapted multi-temporal two-phase burn area (BA) algorithm. It uses shortwave and near-infrared band reflectance measurements from Sentinel-2 MSI and also active fire detections by the Terra and Aqua MODIS sensors. Covering an area of approximately 25 million km<sup>2</sup> in Sub-Saharan Africa, burned areas were detected using this algorithm with a spatial resolution of 20 m from January to December 2016, marking the first high-resolution BA study using Sentinel-2 for such an extensive area.

Llorens et al. [14] developed and applied a technique to estimate the total area damaged by forest fires in Spain and Portugal in October 2017. MODIS (250 m) images were compared with the European Forest Fire Information System (EFFIS) database. Sentinel-2 and EFFIS showed a strong correlation for estimating burn severity as indicated by the separability index (SI) and kappa statistic (k), with all cases having SI values higher than one and k values greater than 0.69. This study concluded that Sentinel-2 dNBR is a suitable alternative to the EFFIS fire parameter, particularly in situations where it's crucial to identify details within the fire itself.

Wang et al. [15] developed a new method involving the Vegetation Difference Index (VDI) and Burn Scarring Index (BSI) models for calculating burned crop areas. The VDI model can significantly reduce the confusing effect of background information related to vegetation (forests and grasslands), water bodies, and buildings. The combination of VDI and BSI allows for the reduction of the influence of non-agricultural information by VDI, thus enhancing the accuracy and speed of the BSI model. The effectiveness of the VDI and BSI models was tested for a winter wheat planting area in Central China.

Ramo et al. [16] evaluated how four widely used remote sensing classification algorithms—Random Forest (RF), Support Vector Machine (SVM), Neural Networks (NN), and a well-known decision tree method (C5.0)—performed. Over 130 Landsat images were used to compile a database of burned and unburned pixels for training purposes. Due to the burned class constituting less than one percent of the total, the resulting database was found to be highly imbalanced. RF showed the best performance compared to reference data for the remaining regions (Angola, Sudan, and South Africa). In a study analyzing forest fires in the Manavgat region of Antalya province in 2021, Arıkan et al. [17] used the Burned Area Index (BAI), Relative Burn Ratio (RBR), Normalized Burn Ratio (NBR), Modified Soil Adjusted Vegetation Index (MSAVI), Normalized Vegetation Index (NDVI), and Soil Adjusted Vegetation Index (SAVI). Subsequently, Machine Learning (ML) classification tools such as Random Forest (RF) Algorithm, Support Vector Machine (SVM), and Classification Regression Tree (CART) were used to rank the data. The results

showed that the Random Forest (RF) was the most accurate algorithm with an overall accuracy of 98.57%, while Support Vector Machines (SVM) were the least accurate method.

Seydi et al. [18] utilized the Deep Siamese Morphological Neural Network (DSMNN-Net) architecture, whose main theme is change detection. The proposed network integrates multi-scale convolution layers with morphological layers to generate deep features. The effectiveness of this approach was evaluated on two fire-damaged areas in Australian forests. The method, using multispectral Sentinel-2 and hyperspectral PRISMA datasets, found a general accuracy index of 98% and a Kappa value over 0.9.

Belenguier-Plomer et al. [19] mapped burned areas (BA) using a deep learning approach that includes radar and optical data from Sentinel-1 and Sentinel-2 sensors. The observed land cover class and data type were primary criteria to determine the optimal CNN size and data normalization method. Using a well-defined CNN within a joint active/passive data combination, a DC value of 0.57 was found for Sentinel-1 and a DC of 0.7 for burned area mapping based on Sentinel-2, similar to or slightly higher in accuracy than previous approaches based on Sentinel-2.

A multitude of methods have been developed to identify burned areas using satellite images. Most of these solutions require time-consuming preprocessing, and deep learning approaches have not yet been extensively explored [20]. Knopp et al. [20] combined current advancements in sensor technology and techniques to provide an autonomous process chain for burned area segmentation based on deep learning. A U-Net architecture was used to train a convolutional neural network (CNN). The final segmentation model had a general accuracy of 0.98 and a kappa correlation of 0.94. Arruda et al. [21] developed a new method for mapping burned areas in Brazil's Cerrado region using a Deep Learning algorithm to analyze Landsat images via Google's Earth Engine and Cloud Storage. The mapped areas were compared with the INPE Burned Area Product (30 m resolution) and the MODIS MCD64A1 Burned Area Product (500 m resolution), finding an accuracy rate of 97%.

Hu et al. [22] demonstrated how deep learning (DL) models can autonomously map burned areas using single-time multi-band images. Sentinel-2 and Landsat-8 data were evaluated using machine learning techniques, and according to validation results, DL algorithms outperformed machine learning approaches. This study showed that combining contextual information from fire-sensitive spectral bands and geographic data allows deep learning algorithms to map burned spots effectively.

Ghali and Akhloufi [23] provided a comprehensive review of deep learning models, emphasizing the effectiveness of CNNs, U-Net, and LSTMs for fire monitoring. Their findings indicate that CNN-based architectures achieve superior accuracy in fire detection, while hybrid models such as CNN-LSTM offer improved wildfire spread prediction.

In addition to these remote sensing-based methods, recent research highlights the increasing effectiveness of deep learning methods in promptly and accurately detecting forest fires. Within this context, Sathishkumar et al. [24] integrated a "Learning Without Forgetting" (LwF) approach into deep learning-based image classification models, proposing a novel framework for forest fire and smoke detection. Their study employed various pre-trained convolutional neural network (CNN) architectures, including VGG16, InceptionV3, and Xception, achieving an accuracy rate of approximately 98.72% with the Xception model. Furthermore, to address the issue of "catastrophic forgetting"—the loss of previously acquired knowledge when models are trained on new data—the authors utilized LwF. This technique not only preserved the performance on the original dataset but also yielded high accuracy on an additional fire/smoke dataset (BoWFire). As a result, this method effectively maintains performance on previously learned tasks while also learning new tasks, thereby enhancing both the accuracy and generalization capability of forest fire detection [24].

Chen et al. [7] conducted a comparative study using Sentinel-1B and 2A imagery and found that the Support Vector Machine (SVM) achieved the highest accuracy (93.52%) in the pre-fire period when combined with spectral and NDVI indices, whereas the Random Forest (RF) algorithm outperformed others during the fire event, reaching an overall accuracy of 95.43% when utilizing spectral and Normalized Burn Ratio (NBR) features. Moreover, in the post-fire stage, SVM again exhibited superior performance (94.97%) when incorporating spectral and radar backscatter coefficients, underscoring the importance of selecting optimal machine learning algorithms for different fire periods.

### 3. MATERIALS AND METHODS

#### 3.1. Study Area

In this study, the forest fire that occurred in the Samandağ region of Hatay between September 5 and 10, 2020, was analyzed, as shown in Figure 1. Information on the fire-affected areas was obtained from the Ministry of Agriculture and Forestry and utilized in this research.

According to the Ministry's reports, the fire in the Yeniköy area of the Samandağ district, Hatay province, was brought under control after five days. High temperatures and low humidity were among the key factors that exacerbated the fire's spread. These environmental conditions not only influenced fire behavior but also played a crucial role in shaping the strategy and effectiveness of the firefighting efforts. Given the impact of such factors, accurate post-fire analysis is essential for understanding the severity of the fire and guiding future prevention measures.

To achieve this, remote sensing techniques were utilized to detect and analyze the burned areas. Fire indices, such as the Normalized Burn Ratio (NBR), offer valuable insights by highlighting changes in vegetation and soil conditions due to fire. These indices are particularly useful in assessing the extent and intensity of the damage in a quantitative manner, providing a clearer understanding of the affected area.

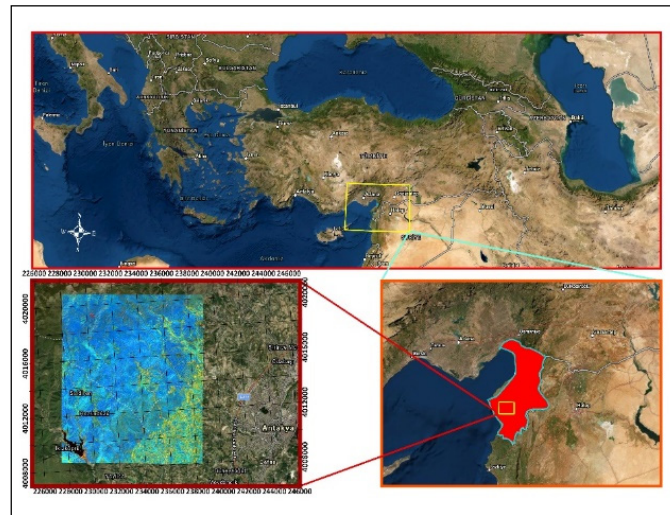


**Figure 1.** Samandağ study area

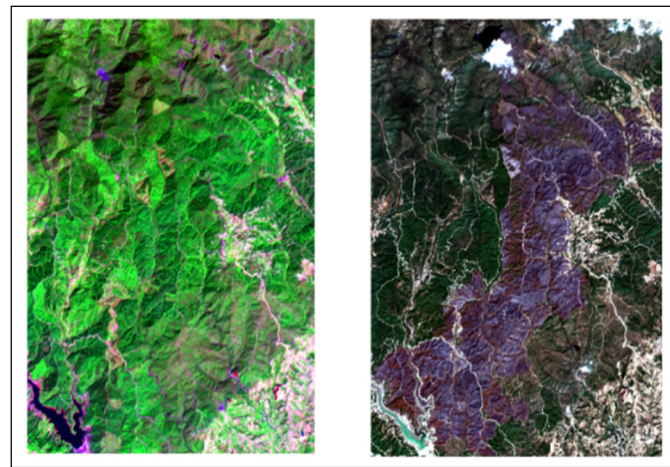


**Figure 2.** Samandağ fire satellite data before and after

In Figure 2, the differences between the pre-fire and post-fire satellite data are easily noticeable, with the burned areas clearly distinguishable in dark brown on the second image.

### 3.1.1. Fire Indices Used During Fire Area Detection

#### 3.1.1.1. NBR and dNBR

The Normalized Burn Ratio (NBR) utilizes Near-Infrared (NIR) and Short-Wave Infrared (SWIR) bands and is sensitive to changes in live vegetation, moisture content, and specific soil conditions [10]. Thus, the NBR index is used for detecting burned areas, and it is expressed using mathematical formulas derived from NIR and SWIR bands [10,25]. The value range for the NBR index spans from -1 to +1.

$$NBR = \frac{(NIR-SWIR)}{(NIR+SWIR)} \quad (1)$$

To classify the severity of burned areas, the difference Normalized Burn Ratio (dNBR or  $\Delta NBR$ ) index is used, which is calculated by subtracting the pre-fire NBR index values from the post-fire NBR index values [26]. This index provides a clear distinction in the severity of the fire impact.

The dNBR formula is expressed as:

$$\Delta NBR = NBR (Pre_{fire}) - NBR (Post_{fire}) \quad (2)$$

The use of dNBR is particularly effective because it quantifies the changes in reflectance characteristics before and after a fire, reflecting the degree to which the fire has altered the landscape. A higher dNBR value typically indicates greater fire severity, as more vegetation loss and soil exposure or charring are detected. The dNBR values are classified into categories to represent different levels of burn severity, from low to high, which helps in planning restoration activities and evaluating fire management effectiveness [10]. This method is widely utilized in ecological studies and forest management to assess fire damage and monitor the ecological recovery of burned areas over time.

Theoretically, the range of the difference Normalized Burn Ratio (dNBR) should be between -2 and +2, but in practice, the range most commonly associated with burned areas is between 0.1 and 1.35. Areas that are unburned typically exhibit dNBR values between -0.1 and 0.1 [27,28].

#### 3.1.1.2. BAIS2 and dBAIS2

Filipponi developed a new approach called BAIS2 (Burned Area Index for Sentinel-2) based on the rich band resolution provided by Sentinel-2 data, accurately detecting burned areas [11]. This method was first employed by Filipponi in 2018. It is calculated using the following formula:

$$BAIS2 = \left( 1 - \sqrt{\frac{B6+B7+B8A}{B4}} \right) * \left( \frac{B12-B8A}{\sqrt{B12+B8A}} + 1 \right) \quad (3)$$

Where B4 (0.665  $\mu\text{m}$ ), B6 (0.740  $\mu\text{m}$ ), B7 (0.783  $\mu\text{m}$ ), B8A (0.865  $\mu\text{m}$ ) and B12 (2.190  $\mu\text{m}$ ) are the spectral bands of the Sentinel 2 satellite image [29].

$$BAIS2(dBAIS2) = BAIS2(Pre_{fire}) - BAIS2(Post_{fire}) \quad (4)$$

The BAIS2 value range for burn signs is from -1 to 1, while the range for actively burning flames is from 1 to 6. It is possible to choose between various BAIS2 value thresholds to reflect various fire intensity densities. The available numbers have been chosen as they have been found to offer consistent results for fires in locations mostly located in the Mediterranean Sea.

#### 3.1.1.3. NDWI

The Normalized Difference Water Index (NDWI), developed by McFeeters, is a tool used to enhance the detectability of water bodies in satellite imagery by leveraging the differential reflectance in the green and near-infrared (NIR) bands [30,31]. This index effectively distinguishes water by increasing the reflection amount in the green band and decreasing it in the NIR band, making water bodies stand out due to their unique spectral properties.

The formula for calculating NDWI is as follows:

$$NDWI = \frac{(Green-NIR)}{(Green+NIR)} \quad (5)$$

Where "Green" refers to the wavelength range that covers green light, and "NIR" denotes the near-infrared spectrum. For the Sentinel-2 satellite, the Green is represented by Band 3 (B3), and NIR by Band 8 (B8) [32,33].

The NDWI values range from -1 to 1, with positive values typically indicating the presence of water. This index is particularly valuable for creating water masks in remote sensing applications, enabling the straightforward exclusion of water areas from land analysis. In your study, the NDWI index was utilized to identify water areas, which were easily masked out from the rest of the imagery, facilitating the focus on terrestrial features and phenomena without the interference of water bodies. This method is crucial for accurate environmental monitoring and management, particularly in areas where water presence significantly influences the ecological or hydrological dynamics.

### 3.2. Method

#### 3.2.1. Obtaining Satellite Images

Satellite data of the study areas were obtained by downloading Sentinel 2D satellite images from the Copernicus Open Access Hub of the European Space Agency (<https://scihub.copernicus.eu>). The closest time to the fire events and the clearest satellite images in terms of cloud cover were selected. The pre-fire and post-fire

Sentinel 2D satellite images of Samandağ study areas were selected and downloaded from the European Space Agency open access data.

**Table 1** Study area satellite data

Study area	Satellite image	Percent cloudiness (%)	Image acquisition date
Samandağ	S2B_MSIL2A_20200828T081609_N0214_R121_T36SYF	6.622	28/08/2020
Study area	S2B_MSIL2A_20200917T081609_N0214_R121_T36SYF	12.727	17/09/2020

Satellite data for the study areas are given in Table 1 Image acquisition dates and cloudiness percentages of the data are indicated. Pre-fire and post-fire images were selected to provide the best view of the study area. It was important that there were few areas in the fire areas that would be obstructed by clouds. Clouds and cloud shadows greatly affect the results.

#### 3.2.1.1. Fire Indices Application Steps

##### *Cloud and Water Masking*

In order to minimize classification errors in fire study areas and to obtain accurate Fire indices results, cloud and water masking operations were performed on the images. The effects of the atmosphere should also be taken into account when determining the appropriate ground reflectance value for satellite imagery [26]. These operations were performed with the help of Snap 7.0 application. In order to perform cloud masking in pre-fire and post-fire images, scl\_cloud\_medium\_proba, scl\_cloud\_high\_proba, scl\_thin\_cirrus cloud mask bands from Sentinel 2 band data were collected using the BandMath operator with the Snap 7.0 application, and a new cloud mask was created by specifying areas with pixel values less than 255 as black and pixel points greater than 255 as white in the new image band of the collection.

In the new band created separately for the pre-fire and post-fire images, the image areas containing clouds were defined as white and the other areas were defined as black. Normalized Difference Water Index (NDWI) was used to mask the water areas in the images.

After finding the water areas for the pre- and post-fire images, a new band named "water\_mask" was created. The water\_mask band was then combined with the cloud masks to create a new band named "cloud\_water\_mask".

This band of cloud and water masks was subtracted from the new image while finding the dNBR index.

### ***Image Preprocessing***

The resolution of the thirteen bands that make up the Sentinel-2 products is not the same everywhere. Since many operators do not accept data with bands of different sizes, the first step for us is to resample the bands so that they have the same resolution level. In the sampling process, using the "Resample" operator with the Snap 7.0 application, the images of the study areas were resampled to a resolution of 10 meters using the bilinear sampling method according to B2 at a resolution of 10 meters.

In the second step, the "Subset" operator was used again with the Snap application to cut the previously selected study areas according to a geographic coordinate polygon and by selecting the bands to be used. This operator is used in the process of segmenting a data product along spatial or spectral dimensions. Subsets of the area can be specified by pixel coordinates or a geographic polygon.

During this sampling process, bands B3, B4, B6, B7, B8, B8A, B12, cloud\_mask and water\_cloud\_mask were selected and cut according to a polygon with geographic coordinates created for the study area.

### ***Fire Index Calculations***

Normalized burn rate (NBR) is the most widely used statistic for burn area and burn severity mapping produced from satellite data. In our study, in the first step, NBR and dNBR index values were calculated using pre-fire and post-fire satellite images for fire zone study areas and fire areas were identified and located.

In the second step, the BAIS2 and dBAIS2 indices, called the Burned Area Index for Sentinel-2 developed by Filippini, were calculated for the images of the study areas and fire zones were identified

## **3.2.2. Deep Learning Implementation Steps**

### **3.2.2.1. Image Pre-Processing**

Post-fire satellite images of the fire zones study areas were resampled according to the B2 Band with a resolution of 10 m with the help of snap 7.0 application. For this sampling process, all bands were selected using the "Resample" operator. Unlike the fire index calculations, only the post-fire satellite image was used. In the next step, using the subset operator, the regions previously selected as the study area were cut by selecting all bands (B1, B2, B3, B4, B5, B6, B7, B8, B8A, B9, B11 and B12) according to the polygons with geographic coordinates.

### **3.2.2.2. Creation of Deep Learning Data Set**

In the process of creating the data set for the deep learning model, burnt and unburnt areas were determined by selecting the areas affected by the fire and the areas not damaged by the fire with geographical coordinate polygons with the help of the Snap 7.0 application. The pixels selected with polygons were then cut using the subset operator with the Snap 7.0 application and converted to data in tiff format. Selected areas are clearly seen in Figure 3 500 geographically coordinated polygons from burned areas and 300 from unburned areas were cut and prepared for the data set. The selection of pixels in the data set was made precisely to prevent classification errors.

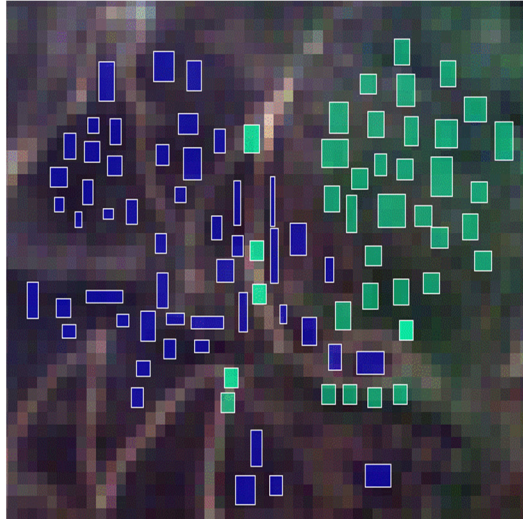


Figure 3. Selection of burnt and unburnt areas

### 3.2.2.3. Creating a Deep Learning Model

The deep learning model was coded in Python programming language using TensorFlow and Keras libraries with Spyder 5.0 application on Anaconda application platform. While creating the deep learning model, we tried to create a model that we can use the data in our study in the most efficient way. The deep neural network model we created is input layer with 12 nodes, 5 hidden layers with 12 nodes per layer and output layer consists of a node. In our model, the data of the satellite image Since 12 bands were resampled after image preprocessing, nodes representing all bands were created in the input layer. Figure 4 shows the model in detail. In the deep learning model, Relu function was used in the hidden layers and sigmoid function was used as activation function in the output layer.

Adam (Adaptive Moment Estimation) optimization was used as the optimization algorithm due to its success and ease of application in updating the weights when working with large data and parameters in deep learning. MSE (Mean Squared Error) was used as the loss function for the losses in the deep learning model.

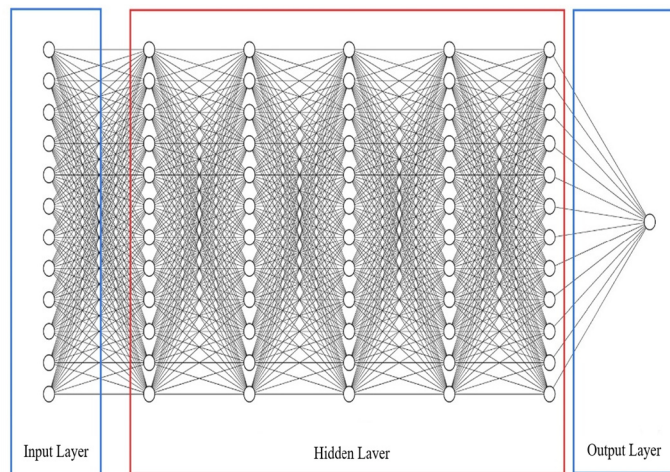


Figure 4. Deep learning model

### 3.2.3. Training and Testing a Deep Learning Model

For training, the images in the previously created dataset were processed using TensorFlow and Keras libraries in the Python programming language and then fed into the deep learning model. The maximum

number of training epochs was set to 300 as the most suitable for our model; however, this value may vary depending on the model architecture and dataset.

To prevent overfitting, an early stopping mechanism was implemented in Python, ensuring that training halts when performance stabilizes. Overfitting can negatively impact model performance by reducing its generalization ability. The dataset was split into 70% for training and 30% for testing to evaluate the model effectively. During testing, the trained model was loaded and tested using a Python-based program, utilizing TensorFlow and Keras libraries once again.

The model's training performance is visualized in Figure 5 and Figure 6. Figure 5 presents the accuracy graph, demonstrating the model's ability to classify burned and unburned pixels. The accuracy improves rapidly in the initial epochs and gradually stabilizes near 1.0, indicating successful learning. Figure 6 depicts the loss graph, representing the pixel-wise classification error between predicted and actual burned/unburned areas. The decreasing loss values over epochs suggest that the model effectively minimizes classification errors. The 'Loss' curve corresponds to the training dataset, while 'val\_loss' represents the validation dataset. Together, these figures confirm the model's convergence and effectiveness in distinguishing burned regions.

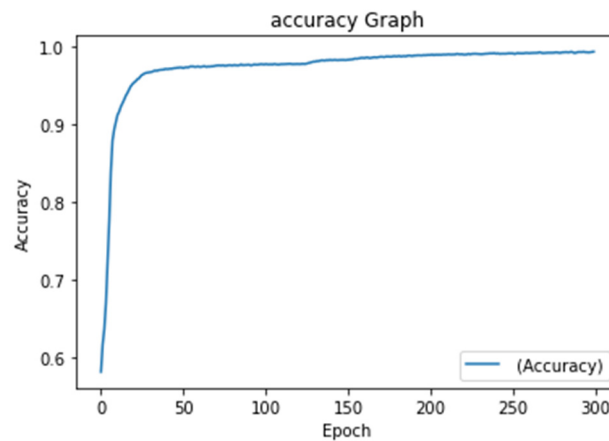


**Figure 5.** Accuracy graph for the training process showing model performance over 300 epochs

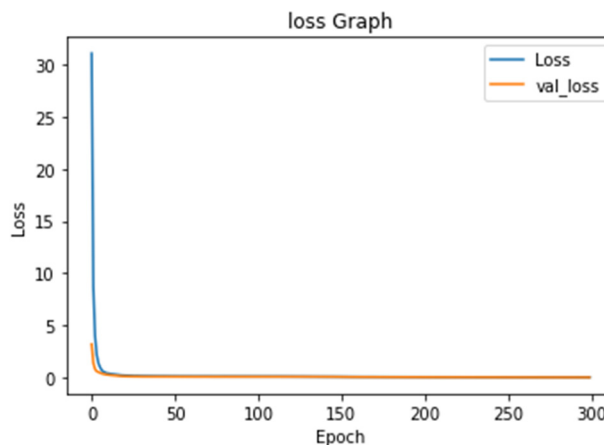


**Figure 6** Loss graph for the training process showing model performance over 300 epochs. The loss represents the pixel-wise classification error between the predicted and actual burned/unburned areas, indicating the model's accuracy in distinguishing between these classes

### 3.2.4. Comparison of Deep Learning and Fire Indices with General Directorate of Forestry Data

In the last step of the study, the deep learning and fire index data were compared with the data in the fire registration slips obtained from the General Directorate of Forestry. The General Directorate of Forestry data was taken as the success criterion. The results of GDF data, fire indices and deep learning method were

evaluated according to their proportional overlap rates. In addition, the data found with ArcGIS PRO 2.7 application were converted into GeoTiff format and mapped spatially on the hybrid map and visually evaluated. Areas outside the fire zones and misclassifications were observed again on the map and their success was evaluated.

## 4. RESULTS AND DISCUSSION

### 4.1. Fire Indexes and Deep Learning Model Results: Samandağ Fire Findings

The images of the study areas were processed according to the dates of occurrence of the fires and fire indices were applied, and then the burned areas were detected with the newly created deep artificial neural network model.

#### 4.1.1. dNBR

The NBR and dNBR indices were first applied for the Samandağ fire, as shown in figure 7. Cloud and water masking were applied to avoid affecting the results of the fire indices.

In the first step, the NBR index was applied on the pre-fire image and then applied on the post-fire image. As a result of these processes, two new bands named NBR (Before Fire) and NBR (After Fire) were formed. The dNBR value was calculated via the new bands and according to the burn severity in the Samandağ study area, the amount of high post-fire regeneration was 14.20 hectares, low post-fire regeneration was 41.85 hectares, unburned area was 9638.20, low burn severity was 789.90 hectares, medium/low burn severity was 582.10 hectares, medium/high burning intensity was found to be 687.30 hectares and high burning intensity was found to be 1880.40 hectares. dNBR results are given in Table 2.

Additionally, Figure 8 provides a detailed visualization of the dNBR index, illustrating the spatial distribution of burn severity (low, moderate/low, and high), helping to assess fire impact.

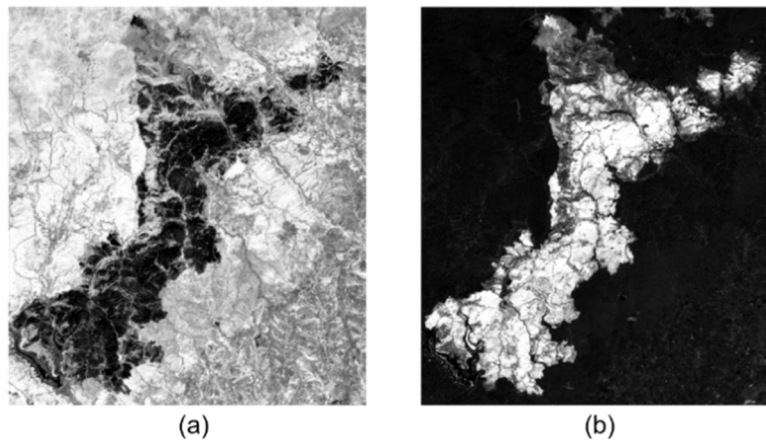


**Figure 7.** Samandağ study area a) NBR index b) dNBR index result

**Table 2.** Samandağ forest fire dNBR index results

Result	dNBR (hectare)
Enchanced regrowth,high(post-fire)	14.20
Enchanced regrowth,low(post-fire)	41.85
Unburned	9638.20
Low severity	789.90
Moderate/Low severity	582.10
Moderate/High severity	687.30
High severity	1880.40

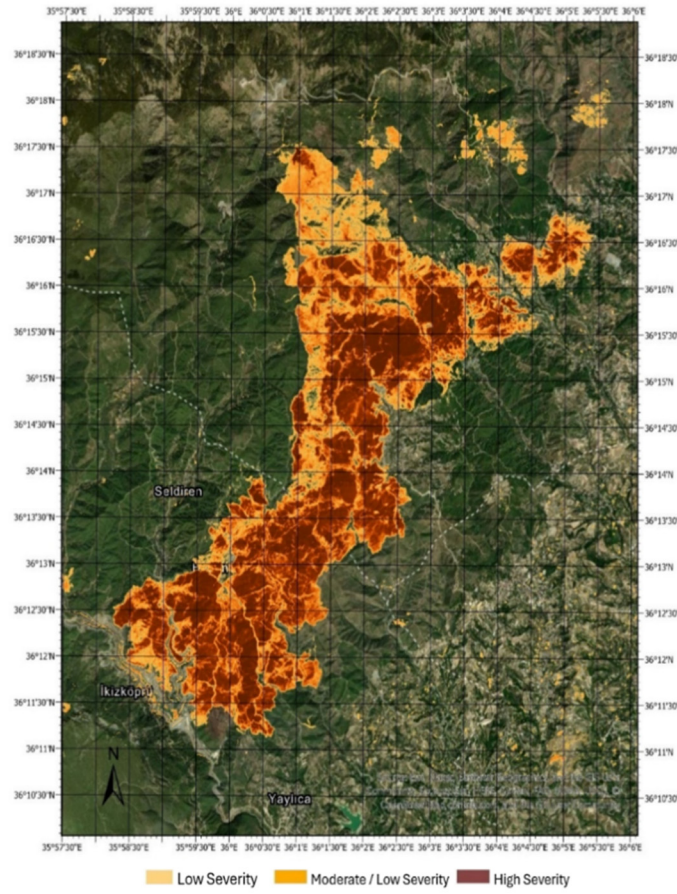


Figure 8. Samandağ study areas DNBR detailed index result

#### 4.1.2. dBAIS2

Calculations for our other fire area identification indices, BAIS2 and dBAIS2, were also performed on pre- and post-fire images, as shown in Figure 9. These calculations generated the BAIS2 (Before Fire) and BAIS2 (After Fire) bands, from which the dBAIS2 index was derived to determine the burned area.

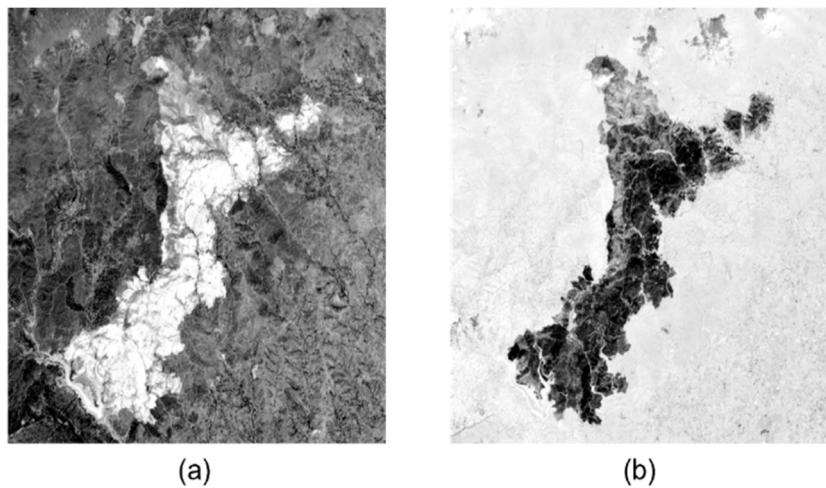


Figure 9. Samandağ study area a) BAIS2 index b) dBAIS2 index result

Figure 10 provides a geographic representation of the burned area, highlighting the extent of fire damage for clearer assessment. According to the dBAIS2 index, a total of 3528.60 hectares of burned land was identified in the Samandağ study area.

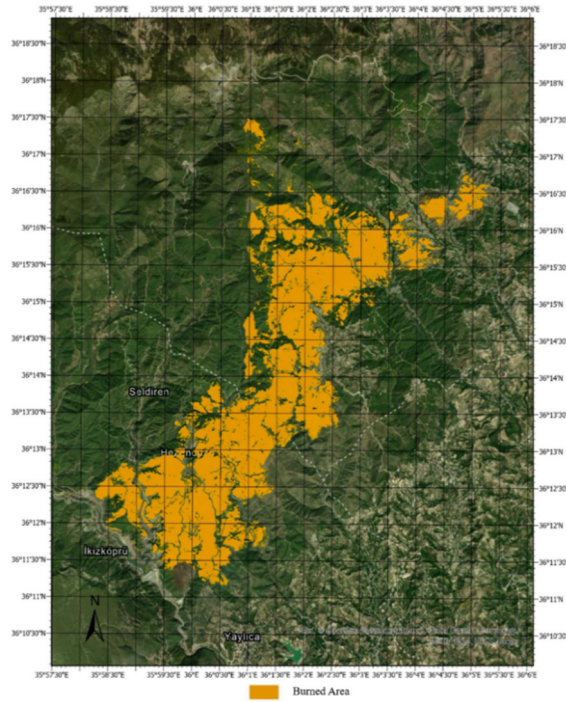


Figure 10. Samandağ study areas detailed dBAIS2 index result

#### 4.1.3. Our Deep Learning Model

With the new deep learning model designed, the image of the study area was classified as burned and unburned areas using the training dataset created with only post-fire data from the Samandağ study area, as shown in Figure 11. The accuracy rate of the new model was found to be 98.36%. According to the results found with the deep learning method, 3605.15 hectares of burned area was identified in the Samandağ study area.

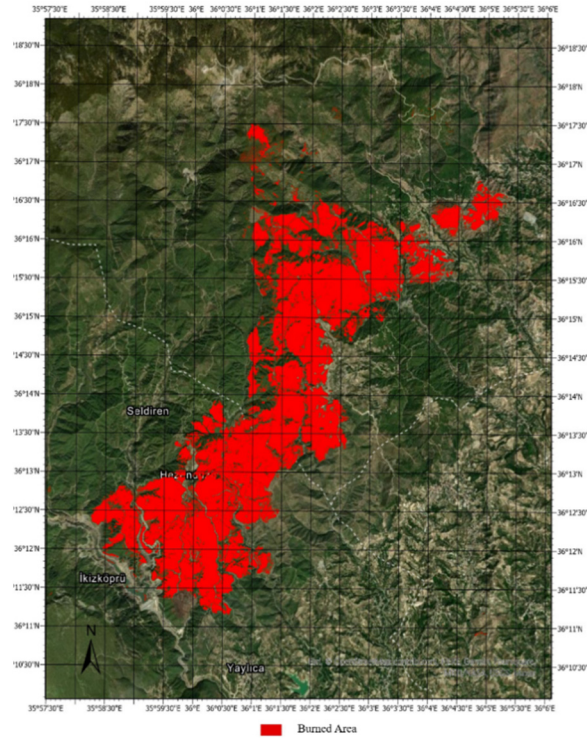


Figure 11. Samandağ region our deep learning model result

For the Samandağ study area forest fire, the dNBR index is 3939.70 hectares, the dBAIS2 index is 3528.60 hectares and 3605.15 hectares of burnt forest area is calculated with the deep learning model. When we look at these values, considering the GDF (General Directorate of Forestry) data, which is 3664.9, as a criterion, dNBR index calculated 274.80 hectares more burned area, dBAIS2 index calculated 136.3 hectares less burned area and deep learning data calculated 59.75 hectares less burned forest area when compared with GDF data. The study area is quite large compared to ordinary fires. dNBR index overlaps 91.50%, dBAIS2 index overlaps 96.28%, deep learning model overlaps 98.36%. According to these values, the fact that the deep learning model finds values closer to the GDF data shows that it provides more consistent and accurate estimates than other indices.

As summarized in Table 3, these values indicate that the deep learning model provides more consistent and accurate estimates compared to other indices.

**Table 2.** Samandağ fire district burning rates

	Samandağ forest fire			
	dNBR index	dBAIS2 index	Deep learning model	General directorate of forestry (GDF) data
Burnt area (Hectare)	3939.70	3528.60	3605.15	3664.9

## 5. CONCLUSION AND SUGGESTIONS

In this study, a new deep learning model was compared with conventional burned area indices (dNBR and dBAIS2) to detect forest fire damage in Hatay's Samandağ region using Sentinel-2 satellite data. The findings demonstrated that the deep learning approach yielded a higher accuracy rate, with a near 98.36% match against the General Directorate of Forestry (GDF) records, surpassing the dNBR and dBAIS2 indices. These results highlight the capacity of deep learning algorithms to more effectively capture and distinguish complex spectral signatures in burned and unburned surfaces, particularly when integrated with Sentinel-2's fine spatial and temporal resolution. By leveraging information from multiple bands, the deep learning model mitigated classification errors more robustly than traditional index-based methods.

The improved accuracy and reliability of the deep learning method bear significant implications for disaster response and forest management. Rapid and accurate assessment of burned areas is critical in devising immediate remediation strategies, guiding reforestation efforts, and optimizing resource allocation during wildfire emergencies. Moreover, the temporal proximity of satellite acquisitions to fire events was crucial in reducing observational gaps; thus, integrating real-time or near-real-time data from drones and ground sensors could further strengthen early detection and damage quantification. Expanding the model's training datasets with diverse geographical regions and vegetation types would also enhance its generalizability. Incorporating a wider range of advanced machine learning architectures, such as convolutional neural networks (CNNs) or attention-based models, could provide even more detailed classifications of burn severity levels and expedite post-fire recovery planning. Consequently, this study underscores the growing importance of deep learning techniques in wildfire monitoring, emphasizing their role in developing more responsive and data-driven forest management policies.

## 6. REFERENCES

1. Sabuncu, A. & Özener, H.A. (2019). Uzaktan algılama teknikleri ile yanmış alanların tespiti: İzmir Seferihisar orman yangını örneği. *Doğal Afetler ve Çevre Dergisi*, 90, 1-9.
2. Özhatay, F., Kültür, Ş. & Gürdal Abamor, B. (2022). Check-list of additional taxa to the supplement of flora of Turkey X. *İstanbul Journal of Pharmacy*, 52, 227-250.
3. Rulli, M.C. & Rosso, R. (2007). Hydrologic response of upland catchments to wildfires. *Advances in Water Resources*, 30, 2072-2086.
4. Fidanboy, M., Adar, N. & Okyay, S. (2022). Derin öğrenmeye dayalı orman yangını tahmin modeli geliştirilmesi ve Türkiye yangın risk haritasının oluşturulması. *Orman Araştırma Dergisi*, 9, 206-218.
5. Sunar, O.N. & Kurnaz, S. (2022). Afet yönetimi bağlamında havacılığın orman yangınlarıyla mücadeledeki rolü üzerine bir değerlendirme. *International Journal of Aeronautics and Astronautics*, 3, 60-70.

6. Adegun, A.A., Viriri, S. & Tapamo, J.R. (2023). Review of deep learning methods for remote sensing satellite images classification: Experimental survey and comparative analysis. *Journal of Big Data*, 10, 93.
7. Chen, X., Zhang, Y., Wang, S., Zhao, Z., Liu, C. & Wen, J. (2024). Comparative study of machine learning methods for mapping forest fire areas using Sentinel-1B and 2A imagery. *Frontiers in Remote Sensing*, 5, 1446641.
8. Chuvieco, E., Martín, M.P. & Palacios, A. (2002). Assessment of different spectral indices in the red–near-infrared spectral domain for burned land discrimination. *International Journal of Remote Sensing*, 23, 5103-5110.
9. Key, C.H. & Benson, N.C. (1999). Measuring and remote sensing of burn severity: The CBI and NBR. In *Proceedings of the Joint Fire Science Conference and Workshop (Vol. II)*, 2, 284.
10. Miller, J.D. & Thode, A.E. (2007). Quantifying burn severity in a heterogeneous landscape with a relative version of the delta normalized burn ratio (dNBR). *Remote Sensing of Environment*, 109, 66-80.
11. Filipponi, F. (2018). BAIS2: Burned area index for Sentinel-2. In *2nd International Electronic Conference on Remote Sensing*, 364.
12. Mpakairi, K.S., Kadzunge, S.L. & Ndaimani, H. (2020). Testing the utility of the blue spectral region in burned area mapping: Insights from savanna wildfires. *Remote Sensing Applications: Society and Environment*, 20, 100365.
13. Tanase, M.A., Belenguer-Plomer, M.A., Roteta, E., Bastarrika, A., Wheeler, J., Fernández-Carrillo, Á. et al. (2020). Burned area detection and mapping: Intercomparison of Sentinel-1 and Sentinel-2 based algorithms over tropical Africa. *Remote Sensing*, 12, 334.
14. Llorens, R., Sobrino, J.A., Fernández, C., Fernández-Alonso, J.M. & Vega, J.A. (2021). A methodology to estimate forest fires burned areas and burn severity degrees using Sentinel-2 data. Application to the October 2017 fires in the Iberian Peninsula. *International Journal of Applied Earth Observation and Geoinformation*, 95, 102243.
15. Wang, S., Baig, M.H.A., Liu, S., Wan, H., Wu, T. & Yang, Y. (2018). Estimating the area burned by agricultural fires from Landsat 8 data using the vegetation difference index and burn scar index. *International Journal of Wildland Fire*, 27, 217.
16. Ramo, R., García, M., Rodríguez, D. & Chuvieco, E. (2018). A data mining approach for global burned area mapping. *International Journal of Applied Earth Observation and Geoinformation*, 73, 39-51.
17. Arıkan, C., Tümer, İ.N., Aksoy, S. & Sertel, E. (2022). Determination of burned areas using Sentinel-2A imagery and machine learning classification algorithms. *2022 4th Intercontinental Geoinformation Days (IGD)*, Tabriz, 43-46.
18. Seydi, S.T., Hasanlou, M. & Chanussot, J. (2021). DSMNN-net: A deep siamese morphological neural network model for burned area mapping using multispectral Sentinel-2 and hyperspectral PRISMA images. *Remote Sensing*, 13, 5138.
19. Belenguer-Plomer, M.A., Tanase, M.A., Chuvieco, E. & Bovolo, F. (2021). CNN-based burned area mapping using radar and optical data. *Remote Sensing of Environment*, 260, 112468.
20. Knopp, L., Wieland, M., Rättich, M. & Martinis, S. (2020). A deep learning approach for burned area segmentation with Sentinel-2 data. *Remote Sensing*, 12, 2422.
21. Arruda, V.L.S., Piontekowski, V.J., Alencar, A., Pereira, R.S. & Matricardi, E.A.T. (2021). An alternative approach for mapping burn scars using Landsat imagery, Google Earth Engine, and deep learning in the Brazilian savanna. *Remote Sensing Applications: Society and Environment*, 22, 100472.
22. Hu, X., Ban, Y. & Nascetti, A. (2021). Uni-temporal multispectral imagery for burned area mapping with deep learning. *Remote Sensing*, 13, 1509.
23. Ghali, R. & Akhloufi, M.A. (2023). Deep learning approaches for wildland fires using satellite remote sensing data: Detection, mapping, and prediction. *Fire*, 6, 192.
24. Sathishkumar, V.E., Cho, J., Subramanian, M. & Naren, O.S. (2023). Forest fire and smoke detection using deep learning-based learning without forgetting. *Fire Ecology*, 19, 9.
25. Cocks, A.E., Fulé, P.Z. & Crouse, J.E. (2005). Comparison of burn severity assessments using differenced normalized burn ratio and ground data. *International Journal of Wildland Fire*, 14, 189-198.
26. Roy, D.P., Huang, H., Boschetti, L., Giglio, L., Yan, L., Zhang, H.H. et al. (2019). Landsat-8 and Sentinel-2 burned area mapping – A combined sensor multi-temporal change detection approach. *Remote Sensing of Environment*, 231, 111254.

27. Key, C.H. & Benson, N.C. (2006). Landscape assessment (LA) sampling and analysis methods. *USDA Forest Service – General Technical Report RMRS-GTR*.
28. Lutes, D.C., Keane, R.E., Caratti, J.F., Key, C.H., Benson, N.C., Sutherland, S. et al. (2006). FIREMON: Fire effects monitoring and inventory system. *Gen. Tech. Rep. USDA Forest Service, RMRS-GTR-164-CD*, 1-55.
29. Han, A., Qing, S., Bao, Y., Na, L., Bao, Y., Liu, X. et al. (2021). Short-term effects of fire severity on vegetation based on Sentinel-2 satellite data. *Sustainability*, 13, 432.
30. McFeeters, S.K. (1996). The use of the normalized difference water index (NDWI) in the delineation of open water features. *International Journal of Remote Sensing*, 17, 1425-1432.
31. Fisher, A., Flood, N. & Danaher, T. (2016). Comparing Landsat water index methods for automated water classification in eastern Australia. *Remote Sensing of Environment*, 175, 167-182.
32. Fernández-García, V., Beltrán-Marcos, D., Fernández-Guisuraga, J.M., Marcos, E. & Calvo, L. (2022). Predicting potential wildfire severity across southern Europe with global data sources. *Science of the Total Environment*, 829, 154729.
33. Zhang, T., Su, J., Liu, C., Chen, W.H., Liu, H. & Liu, G. (2017). Band selection in Sentinel-2 satellite for agriculture applications. *2017 23rd International Conference on Automation and Computing (ICAC)*, Huddersfield, 1-6.